J|A|C|S
ARTICLES
Published on Web 09/12/2006

Molded, High Surface Area Polymer Electrolyte Membranes from Cured Liquid Precursors

Zhilian Zhou,[†,‡] Raymond N. Dominey,[§] Jason P. Rolland,[†,‡] Benjamin W. Maynor,[†,‡] Ashish A. Pandya,[†,‡] and Joseph M. DeSimone*[,†,‡,||]

Contribution from the Department of Chemistry and the Institute for Advanced Materials, Nanoscience and Technology, University of North Carolina at Chapel Hill, Chapel Hill, North Carolina 27599, NSF Science and Technology Center for Environmentally Responsible Solvents and Processes, Department of Chemistry, University of Richmond, Richmond, Virginia 23173, and Department of Chemical and Biomolecular Engineering, North Carolina State University, Raleigh, North Carolina 27695

Received June 21, 2006; E-mail: desimone@unc.edu

Abstract: Polymer electrolyte membranes (PEMs) for fuel cells have been synthesized from easily processable, 100% curable, low molecular weight reactive liquid precursors that are photochemically cured into highly proton conductive solid membranes. The liquid precursors were directly cured into membranes of desired dimensions without the need for further processing steps such as melt extrusion or solvent casting. By employing chemical cross-linking, high proton conductivities can be achieved through the incorporation of significant levels of acidic groups without rendering the material water-soluble, which plagues commonly used non-cross-linked polymers. Fabrication of membrane electrode assemblies (MEAs) from these PEMs resulted in fuel cells that outperformed those based on commercial materials. Moreover, these liquid precursors enabled the formation of three-dimensional, patterned PEMs with high fidelity, micron-scale features by using soft lithographic/micromolding techniques. The patterned membranes provided a larger interfacial area between the membrane and catalyst layer than standard flat PEMs. MEAs composed of the patterned membranes demonstrated higher power densities over that of flat ones without an increase in the macroscopic area of the fuel cells. This can potentially miniaturize fuel cells and promote their application in portable devices.

1. Introduction

Fuel cells are devices that convert the chemical energy stored in a fuel directly into electricity. As a potential candidate for environmentally benign and highly efficient power generation technology, fuel cells are attracting increasing interest.[1−3] The simplicity in design and in operational properties makes polymer electrolyte membrane (PEM) fuel cells ideal as power sources for portable electronic devices, passenger vehicles, and distributed power generation, where high power-to-weight ratios and fast start-up times are needed. The PEM serves as the electrolyte for transport of protons from the anode to the cathode while maintaining a barrier to keep the fuel and the oxidant separate.[4] For a fuel cell to work effectively and to be widely adapted, the PEM must have a portfolio of properties including acceptable costs, high proton conductivity, good chemical and thermal stability, good mechanical strength, and low fuel crossover.[5]

The current state-of-the-art PEM material is Nafion, a perfluorinated ionomer membrane developed by DuPont. To prepare such a perfluorinated membrane, unsaturated monomers of tetrafluoroethylene (TFE) and perfluoro(4-methyl-3,6-dioxa-7-octene-1-sulfonyl fluoride) (PSEPVE) are copolymerized by a free radical initiated reaction. The copolymer is then extruded in the melt processable sulfonyl fluoride form to form a membrane with certain thickness, which is later converted to the acid form by base hydrolysis and acid treatment. Dispersions of Nafion can be obtained by heating the polymer in mixtures of water and alcohol at 240 °C in an autoclave under pressure.[6] Such dispersions can be dried to form the so-called "recast" Nafion membranes, whose morphology and physical properties are different from the extruded membranes. As the gold standard PEM material, Nafion has many desirable properties such as good chemical and thermal stability, high proton conductivity under conditions of high water availability and reasonable mechanical properties. However, Nafion has several shortcomings that limit its utility and performance such as high synthesis

[†] University of North Carolina at Chapel Hill.
[‡] NSF Science and Technology Center for Environmentally Responsible Solvents and Processes.
[§] University of Richmond.
[||] North Carolina State University.

(1) Appleby, A. J.; Foulkes, R. L. *Fuel Cell Handbook*; Van Nostrand Reinhold: New York, 1989.
(2) Whittingham, M. S.; Savinell, R. F.; Zawodzinski, T. A. *Chem. Rev.* **2004**, *104*, 4243−4244.
(3) Malhotra, S.; Datta, R. J. *J. Electrochem. Soc.* **1997**, *144*, L23−L26.
(4) Minh, N. Q. In *Electronic Materials Chemistry*; Pogge, H. B., Ed.; Marcel Dekker: New York, 1996.
(5) Hickner, M. A.; Ghassemi, H.; Kim, Y. S.; Einsla, B. R.; McGrath, J. E. *Chem. Rev.* **2004**, *104*, 4587−4612.
(6) Grot, W. G. (E. I. DuPont) US Patent 4,433,082, 1984.

and processing costs,[7] diminished proton conductivity under conditions of low water availability,[8−10] and high fuel crossover when used in direct methanol fuel cells (DMFC).[11] Significant efforts have been devoted worldwide to develop high performance and reliable membranes. Some of the polymer electrolytes investigated to date include sulfonated poly(arylene ether)s,[12] graft[13] or block copolymers[14] based on sulfonated polystyrene (PS), acid-doped polybenzimidazole (PBI),[15] sulfonated poly(imides),[16] and polyphosphazenes.[17] Each of these materials has their own advantages and disadvantages, and Nafion still stands as the state-of-the-art PEM material.

Similar to Nafion, most of the conventional PEM materials are processed into a membrane form by melt extrusion or solvent casting and employed as preformed membranes in membrane electrode assembly (MEA) fabrication. The requirement of using preformed membranes may restrict new fuel cell designs and developments. Holdcroft and co-workers[18] proposed the concept of making PEMs from curable liquid precursors and pointed out that such a liquid-to-PEM approach may enable the formation of PEMs conformable by injection molding, formed as microchannels and unique shapes, or strongly adhering to the catalyst layer without hot pressing. They dissolved a preformed linear proton conducting polymer, sulfonated poly(ether ether ketone) (SPEEK), in a mixture of vinyl monomer and cross-linking agent and polymerized this composition to form a semi-interpenetrating network in which SPEEK stayed as a guest polymer in a statistically cross-linked host polymer matrix. By doing so, they demonstrated the fabrication of 1-mm features using photolithographic techniques. However, such large features are essentially no use for many fuel cell developments, and the guest SPEEK is not chemically attached to the network.

In this work, we present a new strategy for making highly proton conductive PEMs from easily processable, 100% curable, low molecular weight reactive liquid precursors to solid membranes. Highly fluorinated liquid precursors based on styrenically functionalized reactive perfluoropolyethers (sPFPE) were used in conjunction with a fluorinated derivative of sulfonated styrenic (SS) monomers. Chemically cross-linked PEMs with desired shape and thickness can be easily prepared from the liquid precursors, and no further processing steps are needed. By using imprint lithography/micromolding techniques,[19,20] three-dimensional, patterned PEMs with micron-sized features can be easily fabricated with high fidelity. Up to now, Nafion and other conventional membranes are flat and smooth at the surface and therefore lacking enhanced performance in such surface area-dependent catalytic electrochemical cells. Patterned membranes can provide larger interfacial area between the membrane and catalyst layer. In addition to other issues, such as transport phenomenon, an increase in active surface area without an increase in the geometric volume of the MEA should result in higher power densities, which can lead to the miniaturization of fuel cells.

Moreover, to achieve good proton conductivity, especially at low relative humidity (RH) conditions, PEMs with high acid-loading are highly desirable. For linear polymers, however, high acid loading does yield better conductivities, but also leads to compromised mechanical strength and swelling effects. Indeed at sufficiently high ion exchange capacity (IEC), acid-containing linear polymers can even become water-soluble.[21] To achieve high proton conductivity without the challenges associated with linear polymers, chemically cross-linkable ionomeric systems were proposed, and several systems were studied. Important cross-linking methods included electron beam[22] or γ-irradiation[23] of preformed membranes and cross-linking through inter/intrachain bridging links[24] through the sulfonic acid groups. However, irradiation cross-linking can result in PEMs with nonuniform properties, and the consumption of sulfonic acid groups results in a decrease in ion content of the membrane, which will result in lower proton conductivity. Our sPFPE−SS system is chemically cross-linked through the styrenic end groups of the liquid precursors, and the cross-link density can be controlled by using sPFPE precursors of different molecular weights. By employing such a chemically cross-linked system, PEMs with very high conductivity and good mechanical integrity can be achieved. The fluorinated, 100% curable liquid precursor to PEM approach can potentially enable the miniaturization of fuel cells and many other opportunities for fuel cell developments.

2. Experimental Section

2.1. Materials. Poly(tetrafluoroethylene oxide-*co*-difluoromethylene oxide) (PFPE) α,ω-diol (number-average molecular weight 3800 g/mol) was purchased from Solvay Solexis. 1,1,1,3,3-Pentafluorobutane was

(7) Gil, M.; Ji, X.; Li, X.; Na, H.; Hampsey, J. E.; Lu, Y. *J. Membr. Sci.* **2004**, *234*, 75−81.
(8) Savadogo, O. *J. New. Mater. Electrochem. Syst.* **1998**, *1*, 47.
(9) Gottesfeld, S.; Zawodzinski, T. A. In *Advances in Electrochemical. Science and Engineering*; Alkire, R. C., Gerischer, H., Kolb, D. M., Tobias, C. W., Eds.; Wiley: New York, 2002; Vol. 5.
(10) Si, Y.; Kunz, H. R.; Fenton, J. M. *J. Electrochem. Soc.* **2004**, *151*, A623−A631.
(11) Cruickshank, J.; Scott, K. *J. Power Sources* **1998**, *70*, 40−47.
(12) For example: (a) Wang, F.; Hickner, M.; Kim, Y. S.; Thomas A. Zawodzinski, J.; McGrath, J. E. *J. Membr. Sci.* **2002**, *197*, 231−242. (b) Kim, Y. S.; Wang, F.; Hickner, M.; Mccartney, S.; Hong, Y. T.; Harrison, W.; Thomas A. Zawodzinski, J.; Mcgrath, J. E. *J. Polym. Sci. Part B: Polym. Phys.* **2003**, *41*, 2816−2828. (c) Kerres, J.; Cui, W.; Reichle, S. *J. Polym. Sci. Part A: Polym. Chem.* **1996**, *34*, 2421−2438.
(13) For example: (a) Ding, J.; Chuy, C.; Holdcroft, S. *Macromolecules* **2002**, *35*, 1348-1355. (b) Ding, J.; Chuy, C.; Holdcroft, S. *Adv. Funct. Mater.* **2002**, *12*, 389−394.
(14) For example: (a) Kim, J.; Kim, B.; Jung, B.; Kang, Y. S.; Ha, K. Y.; Oh, I.-H.; Ihn, K. J. *Macromol. Rapid Commun.* **2002**, *23*, 753−756. (b) Mokrini, A.; Acosta, J. L. *Polymer* **2001**, *42*, 9−15. (c) Elabd, Y. A.; Walker, C. W.; Beyer, F. L. *J. Membr. Sci.* **2004**, *231*, 181−188.
(15) For example: (a) Xiao, L.; Zhang, H.; Scanlon, E.; Ramanathan, L. S.; Choe, E.-W.; Rogers, D.; Apple, T.; Benicewicz, B. C. *Chem. Mater.* **2005**, *17*, 5328−5333. (b) Samms, S. R.; Wasmus, S.; Savinell, R. F. *J. Electrochem. Soc.* **1996**, *143*, 1225−1232. (c) Wainright, J. S.; Wang, J. T.; Weng, D.; Savinell, R. F.; Litt, M. *J. Electrochem. Soc.* **1995**, *142*, L121−L123.
(16) For example: (a) Asano, N.; Aoki, M.; Suzuki, S.; Miyatake, K.; Uchida, H.; Watanabe, M. *J. Am. Chem. Soc.* **2006**, *128*, 1762−1769. (b) Miyatake, K.; Zhou, H.; Watanabe, M. *Macromolecules* **2004**, *37*, 4956−4960. (c) Miyatake, K.; Zhou, H.; Matsuo, T.; Uchida, H.; Watanabe, M. *Macromolecules* **2004**, *37*, 4961−4966.
(17) For example: (a) Carter, R.; Wycisk, R.; Yoo, H.; Pintauro, P. N. *Electrochem. Solid-State Lett.* **2002**, *5*, A195−A197. (b) Guo, Q. H.; Pintauro, P. N.; Tang, H.; O'Connor, S. *J. Membr. Sci.* **1999**, *154*, 175−181.
(18) Schmeisser, J.; Holdcroft, S.; Yu, J.; Ngo, T.; McLean, G. *Chem. Mater.* **2005**, *17*, 387−394.
(19) Xia, Y.; Whitesides, G. M. *Angew. Chem. Int. Ed.* **1998**, *37*, 550−575.
(20) Rolland, J. P.; Hagberg, E. C.; Denison, G. M.; Carter, K. R.; DeSimone, J. M. *Angew. Chem. Int. Ed.* **2004**, *43*, 5796−5799.
(21) Kerres, J.; Cui, W.; Reichle, S. *J. Polym. Sci. Part A: Polym. Chem.* **1996**, *34*, 2421−2438.
(22) Miyatake, K.; Zhou, H.; Watanabe, M. *Macromolecules* **2004**, *37*, 4956−4960.
(23) For example: (a) Chen, J.; Asano, M.; Yamaki, T.; Yoshida, M. *J. Membr. Sci.* **2005**, *256*, 38−45. (b) Schmidt, T. J.; Simbeck, K.; Scherer, G. G. *J. Electrochem. Soc.* **2005**, *152*, A93−A97. (c) Bae, B.; Ha, H. Y.; Kim, D. *J. Membr. Sci.* **2006**, *276*, 51−58.
(24) For example: (a) Kerres, J.; Cui, W.; Disson, R.; Neubrand, W. *J. Membr. Sci.* **1998**, *139*, 211−225. (b) Mikhailenko, S. D.; Wang, K.; Kaliaguine, S.; Xing, P.; Robertson, G. P.; Guiver, M. D. *J. Membr. Sci.* **2004**, *233*, 93−99. (c) Kerres, J.; Cui, W.; Reichle, S. *J. Polym. Sci. Part A: Polym. Chem.* **1996**, *34*, 2421−2438.

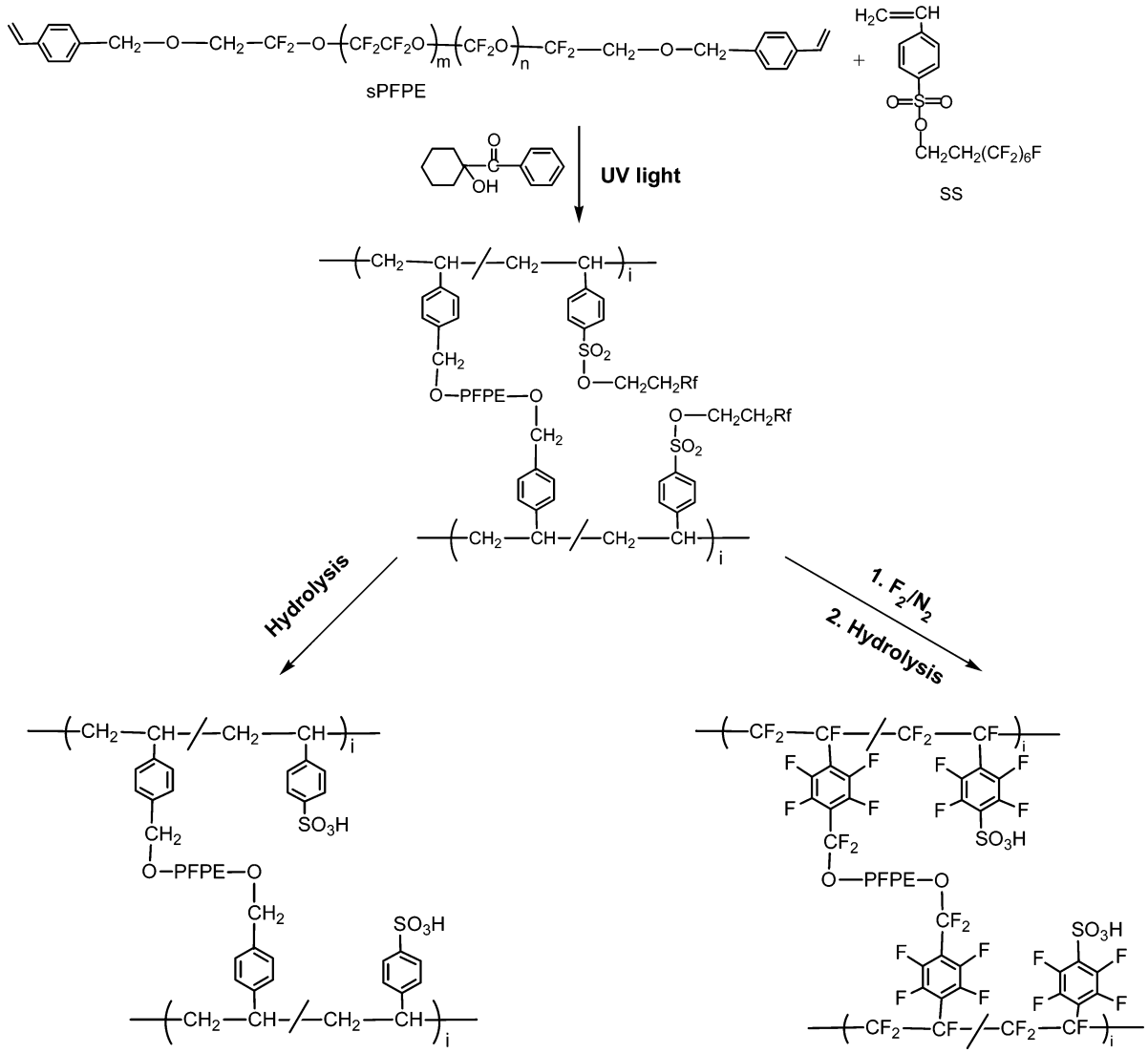

Figure 1. Chemical structures of the precursor materials and the cross-linked PEM materials in H-form.

obtained from Solvay Fluoride. All other chemicals were purchased from Aldrich and used as received.

2.2. Synthesis of sPFPE. In order to incorporate a cross-linkable functionality, a styrene linkage was added to both chain ends of PFPE α,ω-diol by a phase-transfer-catalyzed reaction. In a typical synthesis, PFPE α,ω-diol (30 g, 7.89 mmol), 1,1,1,3,3-pentafluorobutane (30 mL), and tetrabutylammonium hydrogen sulfate (1.5 g, 4.42 mmol) were added into a round-bottom flask. KOH (15 g, 0.27 mol) dissolved in deionized water (30 mL) was then added under stirring. After addition of 4-vinylbenzyl chloride (3 mL, 19.2 mmol), the reaction mixture was allowed to stir vigorously at 45 °C for 48 h. The product was filtered to remove the brown solid, and the resulting solution was washed with deionized water three times and stirred with carbon black for 10 h. The mixture was passed through a 0.22-μm filter to remove the carbon black and vacuum-dried at room temperature to remove the solvent. The resulting product is a clear viscous liquid, whose structure is shown in Figure 1. 400 MHz ^{1}H NMR ($CDCl_3$): δ 3.82 (2H, CF_2CH_2O), 4.65 (2H, $-OCH_2$-$\phi-$), 5.25 and 5.80 (vinyl, $CH{=}CH_2$), 6.75 (vinyl, $CH{=}CH_2$), 7.30−7.50 (4H, aromatic).

2.3. Synthesis of Fluorinated Styrene Sulfonate Monomer. 4-Vinylbenzenesulfonyl chloride was synthesized by the following procedure.[25] Sodium *p*-styrenesulfonate (26.3 g, 128 mmol) was added to thionyl chloride (70 mL) under Ar flow in small portions with stirring. Dry *N*,*N*-dimethylformamide (35 mL) was added to the resulting suspension dropwise. The reaction mixture became homogeneous, and it was stirred for 6 h at room temperature. The reaction mixture was kept in a refrigerator overnight and poured into ice water to quench unreacted thionyl chloride. The aqueous solution was extracted three times with diethyl ether, and the combined ether layer was washed with 10% NaCl solution three times and then dried over $MgSO_4$ for 1 h. $MgSO_4$ was then filtered out and diethyl ether was removed by vacuum evaporation. The resulting product is a yellow liquid and not miscible with PFPE. 400 MHz ^{1}H NMR ($CDCl_3$): δ 5.55 and 5.96 (vinyl, $CH_2{=}CH$), 6.80 (vinyl, $CH_2{=}CH$-ϕ) 7.55−8.05 (4H, aromatic).

In order to make a styrene sulfonic acid precursor that is miscible with PFPE, a fluorocarbon tail was added to 4-vinylbenzenesulfonyl chloride. To a round-bottom flask, 4-vinylbenzenesulfonyl chloride (7.6 g, 37.5mmol), 3,3,4,4,5,5,6,6,7,7,8,8,8-tridecafluoro-1-octanol (13.66 g, 37.5mmol), triethylamine (10 mL), and pyridine (20 mL) were added under Ar flow. The resulting slurry was stirred at room temperature for 20 h. The reaction mixture was then poured into excess hydrochloric acid−ice bath to quench the triethylamine. The aqueous solution was extracted with diethyl ether three times, and the combined ether layer was washed sequentially with water, 10% NaOH solution, and 10% NaCl solution. The ether solution was then dried over $MgSO_4$ for 1 h. $MgSO_4$ was filtered out, and diethyl ether was removed by vacuum

(25) Ishizone, T.; Tsuchiya, J.; Hirao, A.; Nakahama, S. *Macromolecules* **1992**, *25*, 4840−4847.

evaporation. The resulting product, styrene sulfonate (SS) ester, is a waxy yellow solid whose structure is shown in Figure 1. 400 MHz ^{1}H NMR ($CDCl_3$): δ 2.50 (2H, $R_fCH_2CH_2$), 4.30 (2H, $R_fCH_2CH_2O$), 5.50 and 5.90 (vinyl, CH_2=CH), 6.75 (vinyl, CH_2=C*H*-ϕ) 7.55−7.90 (4H, aromatic). 400 MHz ^{19}F NMR ($CDCl_3$); −81 (3F, CF_3), −116 (2F, CF_3CF_2), −122 to −124 (6F, $CF_2CF_2CF_2CF_2CF_2$), −126.5 (2F, $-CF_2CH_2-$).

2.4. Membrane Preparation. To make a membrane, sPFPE with 1 wt % photoinitiator (1-hydroxycyclohexyl phenyl ketone) and SS were mixed in the desired ratio. The mixture was heated above 40 °C to form a homogeneous yellow liquid. The liquid precursor was poured onto a preheated glass slide or a patterned substrate and then chemically cross-linked by irradiation with UV light (λ = 365 nm) for 20 min under nitrogen purge. The resulting solid membrane in the ester form is transparent and slightly yellow.

To prepare patterned membranes without possible damage to the expensive silicon master, a patterned poly(cyanomethyl acrylate) template was prepared by soft lithography techniques. A patterned perfluoropolyether (PFPE) mold was first generated by pouring α,ω-methacryloxy-functionalized PFPE (PFPE−DMA) liquid precursor containing 1 wt % 1-hydroxycyclohexyl phenyl ketone over a patterned silicon master followed by subsequent UV curing under N_2 atmosphere. The fully cured PFPE−DMA mold was then released from the silicon master and had the negative image of the silicon master. Liquid cyano methyl acrylate (CMA) monomers were transferred onto the glass substrate and the PFPE−DMA mold was quickly placed on top of the CMA monomers. Air bubbles in the CMA liquid layer were carefully removed. The apparatus was kept at ambient conditions for 24 h in order for the CMA monomers to polymerize. After the reaction was complete, the poly(cyano methyl acrylate) (PCMA) became a solid polymer, having the same patterns as the silicon master. The PFPE−DMA mold was then removed from PCMA and the glass substrate. At this point, the patterned PCMA polymers were adhered to the glass substrate and used as a template to make patterned sPFPE−SS PEMs.

To further improve the thermal and chemical stability of the partially fluorinated PEM materials, membranes were fluorinated by elemental fluorine gas before hydrolysis (Exfluor). This fluorination process can possibly replace both aliphatic and aromatic hydrogen with fluorine atoms. Membranes in ester form were treated sequentially with N_2 at room temperature for 24 h, 1% F_2 in N_2 at room temperature for 24 h, and N_2 at room temperature for 24 h.

To convert the sulfonate ester groups into sulfonic acid, the membranes were soaked in a 5:6 (v/v) mixture of 30% NaOH aqueous solution and methanol for 12 h and then refluxed in the same mixture for an additional 10 h. After rinsing with distilled water, the membranes were stirred for a total of 24 h in fresh 20 wt % HCl solution, which was refreshed four times. The resulting membranes were in the acid form. Residual HCl was removed by washing with distilled water.

2.5. Molecular Characterization. Nuclear magnetic resonance (NMR) spectra were taken using a Bruker 400 MHz DRX spectrometer. Membranes in the ester and sodium salt forms were analyzed by elemental analysis (Atlantic Microlab).

2.6. Scanning Electron Microscopy. Scanning electron microscope (SEM) images were collected on a Hitachi S4700 SEM. In order to obtain high-quality images, samples were coated with a thin layer of gold (around 10 nm) using a standard sputter-coater (Cressington 108 auto).

2.7. Ion Exchange Capacity Measurement. Equivalent weight (EW) and ion exchange capacity (IEC) of the membranes were determined by titration of the sulfonic acid groups. In a titration measurement, a piece of membrane (typically 0.2−0.3 g) in acid form was stirred with saturated NaCl solution overnight; the resulting solution was then titrated with standardized 0.01 mol/L NaOH solution using phenolphthalein as the indicator. The titrated membrane was in the salt form and dried over phosphorus pentaoxide (P_2O_5) for 1 week at room temperature, at which point it was accurately weighed. The EW and IEC of the membranes are calculated as follows:

$$\mathrm{EW}\ (\mathrm{H}^+, \mathrm{g\ mol}^{-1}) = [\text{dry weight}/(V_{\mathrm{NaOH}} \times [\mathrm{NaOH}])] - 22$$

$$\mathrm{IEC}\ (\mathrm{mequiv\ g}^{-1}) = 1000/\mathrm{EW}$$

2.8. Thermal and Mechanical Analysis. The thermal stability of the membranes was measured by a Perkin-Elmer Pyris 1 thermogravimetric analyzer (TGA). All the samples were heated from room temperature to 120 °C and kept at 120 °C for 1 h to remove residual water. The samples were then cooled down to room temperature and heated to 500 °C in a nitrogen atmosphere with a heating rate of 10 °C/min. The onset of rapid weight loss was defined as the decomposition temperature.

Dynamic mechanical and thermal analysis (DMTA) measurements were performed with a 210 Seiko dynamic mechanical spectroscopy (DMS) instrument, operating at fixed frequency and film tension mode. The frequency used was 1 Hz and the temperature was varied from −140 to 350 °C at a heating rate of 2 °C/min.

The mechanical properties of the PEM materials were measured by an Instron system (model 5566) at ambient conditions (20 °C and 35% relative humidity) using a 10 kN load cell. Samples were equilibrated under these conditions before the measurements were performed. A typical sample size used for these measurements was 20 mm × 5 mm × 0.2 mm. An extensiometer of 15 mm gauge length and a crosshead speed of 10 mm/min were used for all the measurements. From the stress−strain curves, the tensile modulus was obtained. Three replicates were performed for each sample.

2.9. Water Uptake and Dimensional Change. After hydrolysis, the membranes were kept in water for at least 24 h at room temperature. The wet membranes were blotted dry and quickly weighed. The membranes were then dried over P_2O_5 for at least 1 week at room temperature and the dried membranes were weighed again. The water uptake of the membranes expressed as a weight percentage is calculated as follows:

$$\text{water uptake (wt \%)} = (W_{\mathrm{wet}} - W_{\mathrm{dry}})/W_{\mathrm{dry}} \times 100$$

The effect of relative humidity on water uptake was also studied. Typically, the membranes were placed in a humidity chamber at the targeted temperature and relative humidity for at least 14 h and then weighed using an analytical balance in the chamber. The membrane's dimensional change due to water uptake from liquid water was measured in the length/width direction and expressed as the percentage of the dry membrane dimensions.

2.10. Proton Conductivity. Proton conductivity (σ) of the membranes was measured by a four-probe AC impedance method over the frequency range of 1 Hz−1 MHz. Impedance spectra were recorded using Solartron 1287 impedance and Solartron 1255 HF frequency response analyzer. The conductivity cell was designed to ensure that the membrane resistance dominated the response of the system, as demonstrated by Zawodzinski and co-workers.[26] The "window" structure of the cell allowed the membrane to equilibrate in situ. Conductivity measurements under fully hydrated conditions were carried out with the cell immersed in liquid water. All samples were equilibrated in water for at least 24 h before the conductivity measurements. At a given temperature, the samples were equilibrated for at least 30 min before any measurements. Repeated measurements were then taken at that given temperature with 10-min interval until no more change in conductivity was observed.

2.11. MEA Fabrication and Testing. To evaluate the fuel cell performance of the sPFPE−SS membranes, LT 140E-W low-temperature ELAT gas diffusion electrodes (E-TEK, NJ) with a Pt catalyst loading of 5 g/m^2 painted with 5 wt % Nafion dispersion were used to

(26) Zawodzinski, T. A.; Neeman, M.; Sillerud, L. O.; Gottesfeld, S. *J. Phys. Chem.* **1991**, *95*, 6040−6044.

Table 1. Characterization of the sPFPE−SS PEM Materials

IEC (mequiv/cm^3)	IEC (mequiv/g)	EW (g/mol)	water uptake (wt %)	λ (H_2O/SO_3H)	dimensional change (%)	σ at rt (S/cm)
Nafion	0.91	1100	34	21.5	20	0.095
0.90	0.53	1900	14	15	9	0.025
1.41	0.83	1200	26	17	17	0.042
1.89	1.11	900	54	25	24	0.087
2.55	1.50	670	76	28	32	0.134
2.84	1.67	600	87	29	34	0.139
3.09	1.82	550	121	37	44	0.254

achieve the most reproducible results. Membrane electrode assembly was fabricated by sandwiching the PEM and a piece of painted electrode on each side into the fuel cell testing hardware. MEA containing Nafion 117 membrane was prepared and investigated under the otherwise identical conditions for comparison.

To demonstrate the effect of surface area, catalyst ink was prepared from carbon-supported Pt catalyst (0.2 g, 20 wt % Pt on Vulcan XC-72, E-TEK), 5 wt % Nafion dispersion (2.56 g), and distilled water (0.192 g). Water was added dropwise to wet the catalyst, 5 wt % Nafion dispersion was then added dropwise to form the ink. The mixture was stirred for at least 5 h before use. MEA was prepared by painting the catalyst ink onto both sides of the membrane. The catalyst layer with Nafion as the binder did not adhere to sPFPE−SS PEMs as well as to a Nafion membrane due to the different chemistry. But a decent coverage on the membrane surface was obtained. The catalyst loading was about 0.2 mgPt/cm^2 based on the geometrical surface area of the membranes. The painted membrane was then sandwiched between two pieces of ELAT diffusion substrates and fixed in the fuel cell testing hardware.

MEAs were tested in 5 cm^2 single cell testing hardware (Fuel cell Technologies, Inc.) made of graphite plates with gas flow channels. The fuel cell was connected to a test station consisting of a humidifier/gas flow controller unit (Teledyne) and a loadbank (Scribner 890C, Scribner Associates, Inc.). A flow rate 0.1 L/min was used for both anode and cathode. The anode−cell−cathode temperature was set at 50−50−45 °C to obtain 75% relative humidity for this instrument at 50 °C. The MEAs were tested at 50 °C and 75% relative humidity under atmospheric pressure. Data were collected at a rate of 0.1 A/point and 20 s/point.

3. Results and Discussion

3.1. Preparation of Chemically Cross-Linked Membranes. In order to make fluorinated PEM materials, highly fluorinated liquid precursors based on curable perfluoropolyethers (sPFPEs) were used in conjunction with a fluorinated derivative of sulfonated styrenic (SS) monomers (Figure 1). The detailed procedures for the synthesis of these liquid precursors are discussed in the Experimental Section, and their molecular structures were confirmed by NMR. In order to form a homogeneous single-phase mixture with sPFPE, it was necessary to use the fluorinated derivates of the sulfonated styrenic monomers as opposed to using the acid form or the sulfonyl chloride form of the styrenic monomer; otherwise, single phase mixtures were not achievable.

During membrane preparation, the sPFPE and SS precursors were mixed in a certain weight ratio and directly cured into a membrane with desired dimensions. No melt extrusion or solvent casting process is necessary. The membrane was then converted to the acid form by hydrolysis. A series of chemically cross-linked sPFPE−SS membranes were prepared with IEC ranging from 0.50 to 1.82 mequiv/g as summarized in Table 1. It is common for linear PEM materials to dissolve in water if they contain a significant amount of acid groups.[21] In particular, in the synthesis of very high IEC Nafion, competing β-scission processes during polymerization result in such lower molecular weight materials that they are unusable for PEMs. The low equivalent weight (EW < 900) polymers are soluble in many polar solvents.[27] Due to the cross-linked nature, sPFPE−SS PEM with IEC as high as 1.82 mequiv/g remained intact after refluxing in methanol−water mixture for 10 h during hydrolysis.

Hydrocarbon-based linear PEM materials with IEC larger than 2.0 mequiv/g have been reported[28] that do not dissolve in water. However, in comparison of the ion concentration of hydrocarbon- and fluorocarbon-based materials, the density effect should be considered. The density of hydrocarbon-based polymeric materials is typically around 1 g/cm^3 or smaller, while the density of most fluorocarbon materials is larger than 1.5 g/cm^3. For PEM materials, the swelling effect of the membrane and the formation of a continuous hydrophilic domain for good proton conduction are both based on volume. In this case, it is more appropriate to use IEC based on volume expressed in units of milliequivalents per cubic centimeter (mequiv/cm^3). An IEC based on mass can be converted to volume-based IEC by simply multiplying the density of the PEM material. The density of PFPE is 1.8 g/cm^3, and the density of sPFPE−SS membranes is about 1.7 g/cm^3 by a rough mass−volume measurement. Therefore, the IEC range of 0.53−1.82 mequiv/g for the sPFPE−SS membranes corresponds to an ion concentration range of 0.9−3.1 mequiv/cm^3 based on volume.

Due to the presence of aliphatic hydrocarbon moieties, the long-term stability of the cross-linked sPFPE−SS PEMs may be questionable. In an effort to improve the long-term stability of these materials, some membranes were treated with elemental fluorine gas (Figure 1) before hydrolysis to exhaustively fluorinate the membrane. While the majority of the following discussion is focused on the partially fluorinated sPFPE−SS PEM materials, the effects of fluorination on thermal stability is discussed in the next section.

3.2. Thermal and Mechanical Properties. The thermal stability of the membranes was investigated by TGA. Independent of IEC, the acid (H) form of the membranes displayed a thermal decomposition temperature of 290 °C. Compared with the acid-form membranes, samples in sodium (Na) form showed a higher thermal stability with a decomposition temperature of 322 °C. It should be noted that the thermal stability observed under nonequilibrium conditions of TGA experiments might be overestimated to some extent. However, these results suggest that the sPFPE−SS membranes are sufficiently stable within the conceivable temperature range of PEM fuel cell applications up to 120 °C. In order to improve the long-term stability of these partially fluorinated materials, the membranes were fluorinated by elemental fluorine gas. Under the current fluorination conditions, the degree of fluorination depended on the SS content of the cross-linked membrane, presumably due to the higher glass transition temperature of the higher SS content samples. By elemental analysis, it was found that 75, 56, 40, and 35% of the H atoms were replaced by F atoms for samples with 40, 50, 60, and 70 wt % SS, respectively. The fluorinated materials exhibited a significant improvement in

(27) Heitner-Wirguin, C. *J. Membr. Sci.* **1996**, *120*, 1−33.
(28) Wang, F.; Hickner, M.; Kim, Y. S.; Thomas, A. Zawodzinski, J.; McGrath, J. E. *J. Membr. Sci.* **2002**, *197*, 231−242.

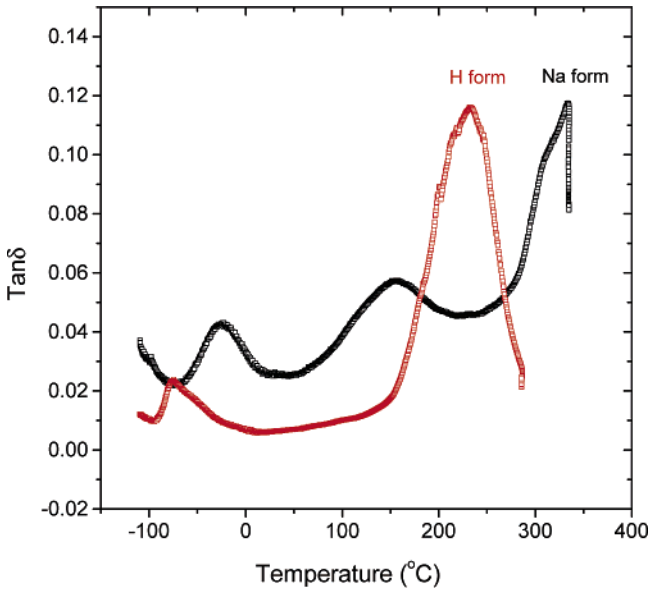

Figure 2. DMTA spectra of sPFPE−SS membranes in H- and Na-forms.

thermal stability, with a decomposition temperature of 359 °C in the sodium form.

DMTA methods have been very useful for the analysis of phase behavior of the polymer studied. While phase separation of cross-linked materials is hard to detect as separate glass transitions by differential scanning calorimetry (DSC), it usually corresponds with clear thermomechanical transitions in DMTA measurements. Thermal transitions of Nafion have been studied by this method. For Nafion in the H-form, an α-transition around 110 °C was observed due to the chain motions within/near the ion-rich domains and a γ-transition at −100 °C was observed due to the short-range molecular motions in the tetrafluoroethylene phase.[29] The effects of counterion type and size on the dynamic mechanical behavior of Nafion were also studied in different ionomer forms such Na^+ or tetrabutylammonium ion.[29]

For the H-form sPFPE−SS PEMs, two transitions were observed in DMTA measurements, one at 200−250 °C (α-transition) and the other at −80 to −45 °C (γ-transition). The α-relaxation is presumably due to chain motions within or/and near the ion-rich domains formed by styrene sulfonic acid, and the γ-relaxation corresponds to chain motions in the sPFPE-rich domains. Compared to typical phase-separated systems such as block copolymers, the sPFPE−SS segment lengths are very short, but these two components would tend to be strongly segregated from each other due to their very different natures. It was found that both IEC values and residual water content affected the peak positions and relative intensities of these two transitions.

As shown in Figure 2, the type of counterion has a very strong effect on the dynamic mechanical properties of the membrane. When converted to the Na-form, the γ-relaxation shifted to slightly higher temperature, and the α-transition shifted significantly to higher temperatures. Since thermal decomposition was observed at 322 °C, we are not sure if the peak observed at 330 °C is the actual α-transition or an artificial peak caused by decomposition. However, an α-transition at higher temperature is expected, since the dipole−dipole interaction between sodium

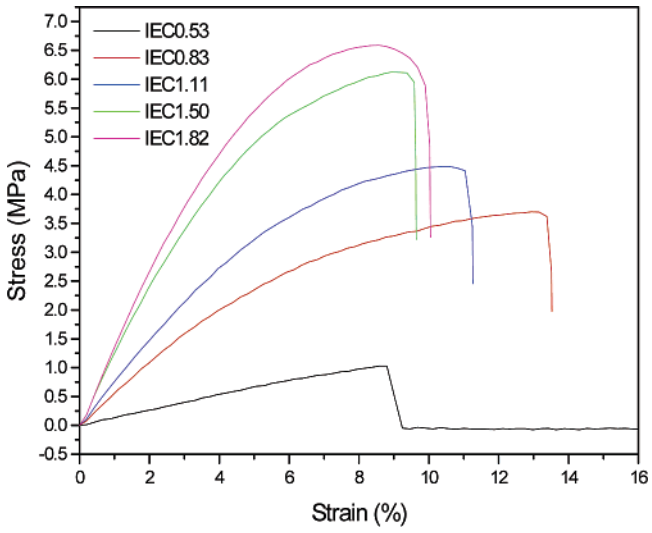

Figure 3. Stress−strain curves of the sPFPE−SS membranes in H-form under ambient conditions (20 °C, 35% RH).

sulfonate groups is much stronger than the hydrogen-bond interaction between the SO_3H groups. In addition, another relaxation near 150 °C was observed for the sodium-form membranes, and this may be associated with the hydrocarbon domains formed mainly by aromatic groups. In the H-form, these two transitions combined together and occurred in the 200−250 °C temperature range.

The mechanical properties of the PEM materials were characterized by an Instron instrument under ambient conditions. Figure 3 shows the stress−strain curves of the membranes in H-form. While the membranes in ester form are elastomeric, the H-form membranes lose their elasticity. Under the testing conditions (20 °C and 35% RH), the membranes became stronger as the ion content increased. As IEC increased from 0.53 to 1.82 mequiv/g, the moduli of the membranes increased from 15 to 126 MPa. Under high RH conditions, high IEC membranes absorbed more water than the low IEC ones, as discussed in the next section. The increased water uptake for higher IEC PEMs could result in a decrease in mechanical strength.

3.3. Water Uptake and Dimensional Change. The water sorption of the polymeric materials has profound effect on the proton conductivity[30,31] and mechanical properties[32,33] of the PEMs. Water uptake of sPFPE−SS membranes from liquid water is presented in Table 1 as the weight percentage of the dry samples and as the number of water molecules per sulfonic acid (λ). The IEC has a strong effect on water uptake. As the IEC changed from 0.53 to 1.82 mequiv/g, the water uptake increased from 14 to 121 wt %. As IEC increases, there are more ionic groups to interact with water. Furthermore, as IEC increases, each ionic group interacts with more water molecules, as indicated by λ. This number increased from 15 water molecules for the IEC 0.53 mequiv/g sample to 37 water molecules for the IEC 1.82 mequiv/g membrane. Without any

(29) Mauritz, K. A.; Moore, R. B. *Chem. Rev.* **2004**, *104*, 4535−4585.
(30) Zawodzinski, T. A.; Neeman, M.; Sillerud, L.; Gottesfeld, S. *J. Phys. Chem.* **1991**, *95*, 6040−6044.
(31) Sanders, E. H.; McGrady, K. A.; Wnek, G. E.; Edmondson, C. A.; Mueller, J. M.; Fontanella, J. J.; Suarez, S.; Greenbaum, S. G. *J. Power Sources* **2004**, *129*, 55−61.
(32) Osborn, S. J.; Moore, R. B. In *230th ACS National Meeting*; American Chemical Society: Washington, DC, 2005.
(33) DuPont. Nafion PFSA Membranes Product Information.

thermal treatment, Nafion 117 (IEC 0.91 mequiv/g) absorbed 34 wt % water from liquid water, corresponding to 21.5 water molecules per acid group.[34]

The membrane's dimensional change along the length/width direction of the sample due to water sorption at fully hydrated conditions is given in Table 1. Analogous to water uptake, dimensional change also strongly depended on IEC values and almost linearly correlated with the water uptake of the membrane. As IEC increased from 0.53 to 1.82 mequiv/g, the swelling ratio increased from 9% to 44%. Under the testing conditions, Nafion 117 displayed a dimensional change of 20%, which agrees with literature results.[35] The sPFPE−SS membranes with IEC 0.83 and 1.11 mequiv/g displayed a dimensional change of 17 and 24%, respectively, which were comparable to that of Nafion. The IEC 1.82 mequiv/g membrane took 121 wt % water from liquid water, which resulted in a 44% dimensional change and loss of mechanical strength of the membrane under fully hydrated conditions. This particular membrane is not suitable for fuel cell applications. For this reason, the 1.67 mequiv/g PEM was selected for the MEA performance tests discussed below.

It is desirable for fuel cells to operate under low relative humidity conditions. The water uptake of Nafion from water vapor at different RH conditions has been well studied.[30,36,37] The water sorption of sPFPE−SS membranes from water vapor was investigated at 25 °C under controlled RH environments. As shown in Figure 4a, all the membranes displayed increased water uptake in a higher RH environment. In the low RH region (RH = 20−65%), there was a relatively small increase in water content with RH. In the high RH region (RH = 65−100%), the increase in water content was steeper than in the low RH region. The low RH region presumably corresponds to uptake of water vapor by the ions in the membrane, while the high RH region may correspond to water that fills the ionic domain and swells the polymer. Similar to water uptake from liquid water, high IEC membranes tend to take more water from vapor than low IEC ones under the same conditions. For example, while the IEC 0.53 mequiv/g membrane took 13 wt % water at 100% RH, IEC 1.82 mequiv/g membrane took as much as 50 wt % water at 100% RH. As indicated by Figure 4b, it can be seen that differences in water uptake between different IEC samples, expressed in terms of weight percentage of the membrane dry weight, are almost completely explained by the difference in ion concentration. When water uptake is expressed as the number of water molecules per sulfonate group (λ), this number looks essentially the same for all the samples at a given RH.

Comparison of water uptake from liquid water and from saturated water vapor (RH = 100%) reveals an apparent paradox. The water sorption of the membrane in equilibrium with water vapor (RH = 100%) is not the same as the water sorption of the same membrane in contact with liquid water. For example, the membrane with IEC = 1.82 mequiv/g sorbs 15 water molecules per sulfonate group from saturated vapor phase vs 37 from liquid phase. A difference in water uptake by

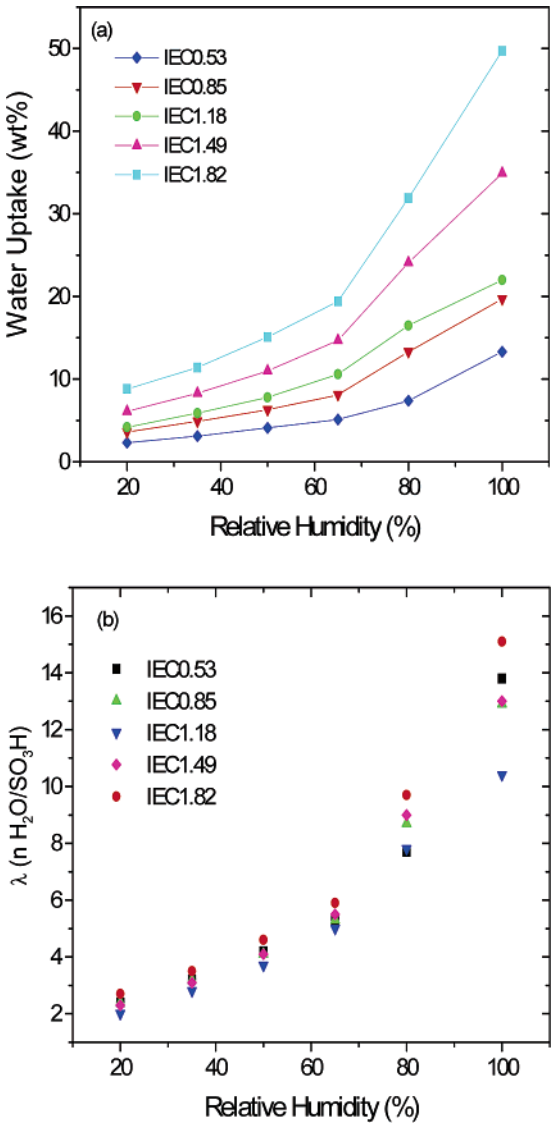

Figure 4. Water uptake of sPFPE−SS membranes from vapor phase with controlled relative humidity (a) in terms of weight percentage and (b) in terms of the number of water molecules per acid group.

polymers from liquid versus saturated water vapor has been observed for several polymer/solvent systems, including Nafion,[9] and is referred to Schroeder's paradox. One explanation is that the polymer surface is more hydrophobic when exposed to water vapor but more hydrophilic when in contact with liquid water. Therefore, water sorption from vapor phase is less favorable.

3.4. Proton Conductivity. In PEM fuel cells, the proton conductivity of the membrane is particularly important, since it plays a significant role in the performance of fuel cells. To achieve good conductivity, high acid loading is desirable. However, for linear PEM materials, this is achieved at the expense of compromised mechanical integrity and excessive swelling. By employing chemically cross-linked systems, we have maximized the acid loading of the PEM materials to achieve higher proton conductivity. Table 1 lists the proton conductivity (σ) of the sPFPE−SS PEMs at room temperature and fully hydrated conditions. As IEC increased from 0.53 to 1.82 mequiv/g, the proton conductivity of the membranes increased by an order of magnitude from 0.025 to 0.254 S/cm. This is reasonable since proton conductivity is determined by the product of charge carrier density and charge carrier mobility

(34) Zawodzinski, T. A.; Derouin, C.; Radzinski, S.; Sherman, R. J.; Springer, T.; Gottesfeld, S. *J. Electrochem. Soc.* **1993**, *140*, 1041.
(35) Vie, P.; Paronen, M.; Stromgard, M.; Rauhala, E.; Sundholm, F. *J. Membr. Sci.* **2002**, *204*, 295−301.
(36) Pushpa, K. K.; Nandan, D.; Iyer, R. M. *J. Chem. Soc. Faraday Trans 1.* **1988**, *84*, 2047−2056.
(37) Randin, J.-P. *J. Electrochem. Soc.* **1982**, *129*, 1215−1220.

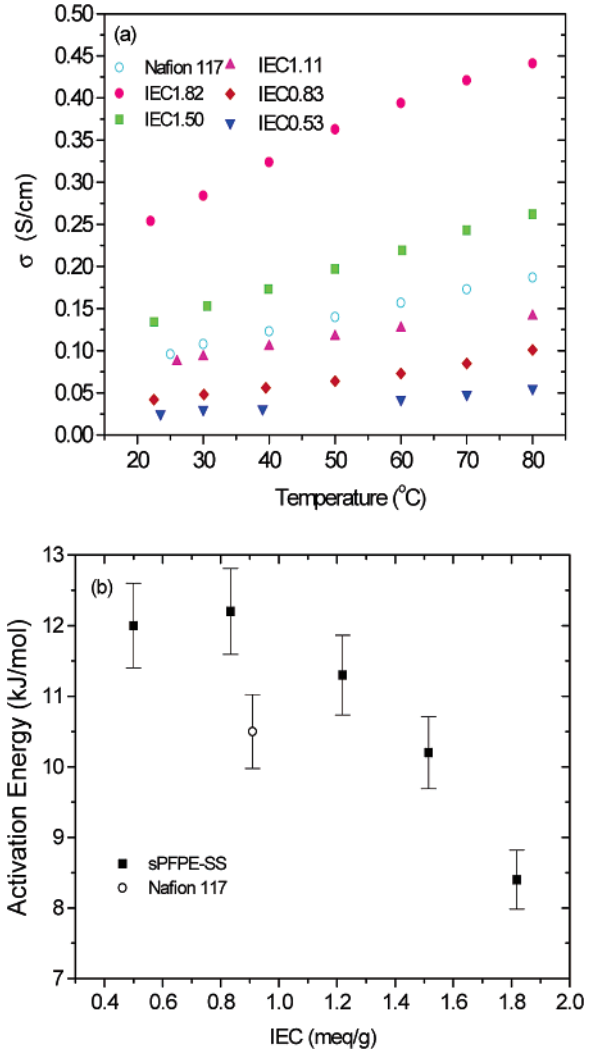

Figure 5. (a) Proton conductivity of sPFPE−SS membranes at different temperatures under fully hydrated conditions and (b) their activation energy for proton conduction.

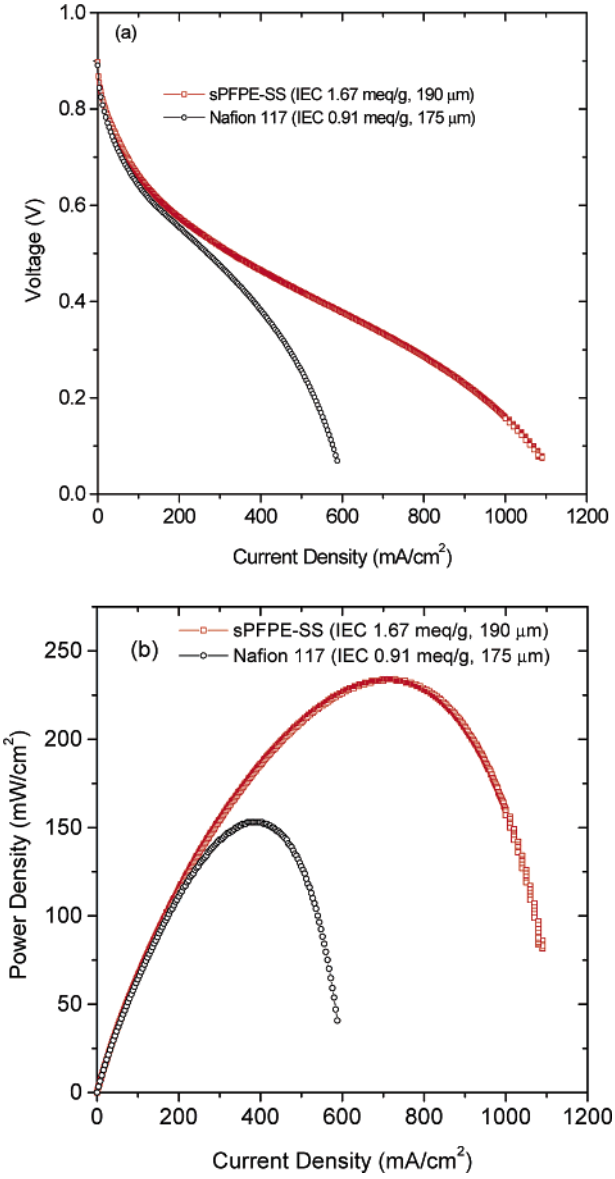

Figure 6. MEA performance of Nafion 117 and sPFPE−SS membrane with a IEC value of 1.67 mequiv/g at 50 °C and 75% RH: (a) polarization curves and (b) power output curves.

and high ion content PEMs have more proton carriers. Nafion 117 has a conductivity of 0.095 S/cm under this condition by our measurement, which agrees well with the literature value. Compared with Nafion, the conductivity of sPFPE−SS membrane with the same IEC is lower. This may relate to the lower pK_a of the sulfonic acid in Nafion and the difference in the morphology and proton mobility of the corresponding PEMs. But the ion loading of Nafion is limited by β-scission during polymerization and the resulting problems with mechanical strength and dissolution in water. By employing a chemically cross-linked system, we can maximize the ion content of membranes and still maintain decent mechanical integrity. The IEC 1.82 mequiv/g membrane has a conductivity of 0.254 S/cm, which is almost 3 times higher than that of Nafion. Many researchers try to design PEM materials that have higher conductivity than Nafion, but not many succeed. For many aromatic-based ionomers, low proton conductivity is observed[38] due to the lack of the formation of properly ordered microphase separation as compared to perfluorinated ionomers.[39] The lower acidity of hydrocarbon-based SO_3H than that of fluorocarbon based SO_3H may also be responsible. The strong hydrophobicity of PFPE in our system may contribute to the formation of microphase separated nanochannels and a conductivity 270% higher than that of Nafion is achieved.

Figure 5 shows the temperature dependence of the proton conductivity and the resultant activation energies for the sPFPE−SS membranes. Similar to many other PEM materials, the proton conductivity of these cross-linked PEMs increased with temperature. According to our measurements, the proton conductivity of both Nafion and the cross-linked sPFPE−SS membranes exhibited Arrhenius behavior. The activation energy (E_a) for the proton conduction in Nafion was measured to be 10.5 kJ/mol, which agrees well with literature values.[40] The activation energy of our cured membranes was found to depend on the IEC values. As shown in Figure 5b, once the ion content

(38) For example: (a) Kopitzke, R. W.; Linkous, C. A.; Anderson, H. R.; Nelson, G. L. *J. Electrochem. Soc.* **2000**, *147*, 1677−1681. (b) Kerres, J.; Cui, W.; Reichle, S. *J. Polym. Sci. Part A: Polym. Chem.* **1996**, *34*, 2421−2438.
(39) Kreuer, K. D. *J. Membr. Sci.* **2001**, *185*, 29−39.
(40) Kim, Y. S.; Wang, F.; Hickner, M.; Mccartney, S.; Hong, Y. T.; Harrison, W.; Thomas, A. Zawodzinski, J.; Mcgrath, J. E. *J. Polym. Sci. Part B: Polym. Phys.* **2003**, *41*, 2816−2828.

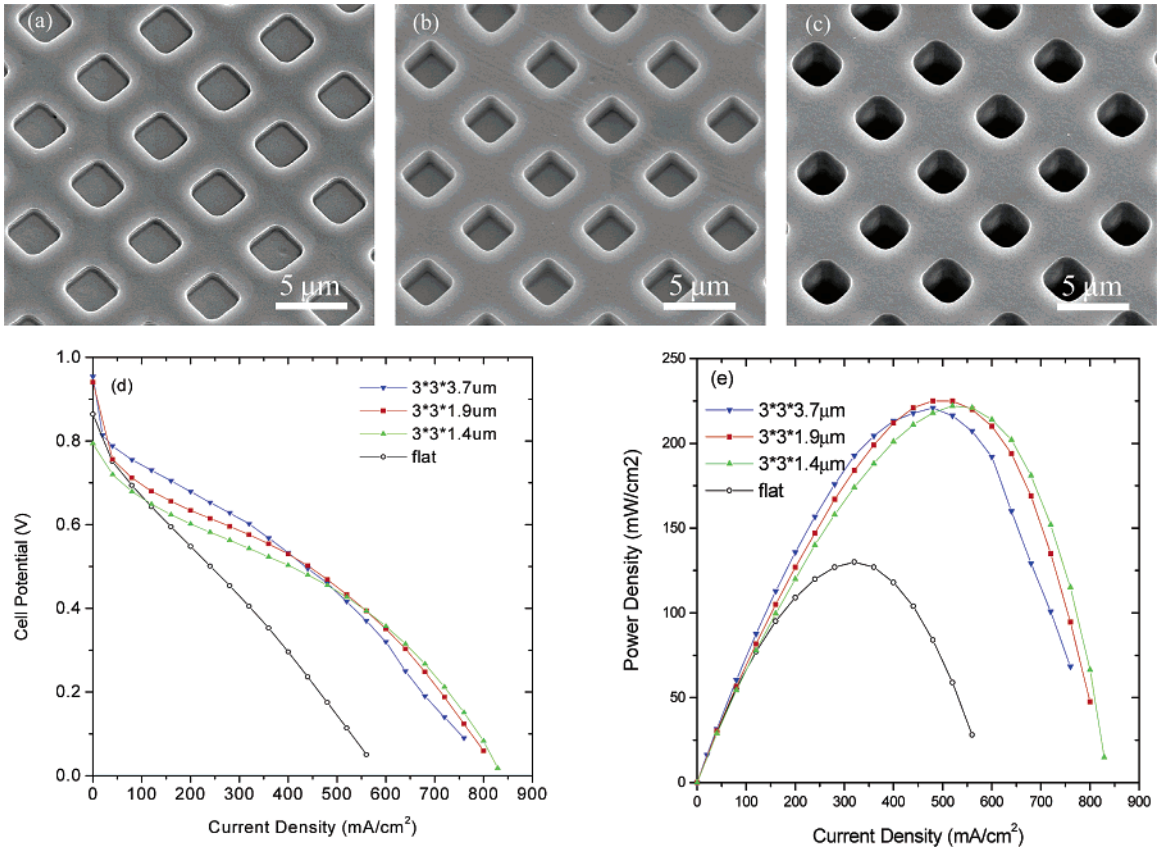

Figure 7. SEM pictures of patterned membranes with feature dimensions (a) 3 × 3 × 1.4 μm, (b) 3 × 3 × 1.9 μm, (c) 3 × 3 × 3.7 μm and MEA performance of patterned and flat sPFPE−SS PEMs with an IEC value of 1.50 mequiv/g and thickness of 190 μm at 50 °C and 75% RH; (d) polarization curves and (e) power output curves.

increased above a certain threshold, the activation energy started to decrease as the IEC increased. Although the proton conduction mechanism and the morphology of the sPFPE−SS membranes are not well understood, we suspect that the decreasing activation energy may be caused by the larger volume fraction of the hydrophilic styrene sulfonic acid component for higher IEC membranes and the easier formation of a continuous network of the ionic domains. The activation energy for proton conduction of the IEC 1.82 mequiv/g sample is 8.4 kJ/mol. Such a low E_a value is very close to that of the Grotthuss mechanism. Since the membrane has a high concentration of sulfonic acid groups and each acid group absorbs as many as 37 water molecules, we suspect that in such high IEC membranes, protons migrate predominantly via the Grotthuss mechanism. Further studies on the membrane morphology by scattering and microscopy techniques and investigations on proton transport mechanisms are under investigation.

3.5. MEA Performance. To investigate the effect of highly proton conductive PEMs on fuel cell performance, MEAs were prepared from our cured PEMs and were compared with MEAs fabricated from Nafion 117 PEMs. Gas diffusion electrodes (LT 140E-W low-temp ELAT, E-TEK, NJ) with a Pt catalyst loading of 5 g/m^2 were used for all of the MEAs in order to make comparisons between the tested systems. Figure 6 shows the MEA performance of Nafion 117 (175 μm thick) and a cured sPFPE−SS membrane with an IEC value of 1.67 mequiv/g (190 μm thick) at 50 °C and 75% RH. Even though the tested sPFPE−SS membrane was thicker than Nafion 117, and the ELAT electrodes were developed and optimized for Nafion-based systems, the MEA made from our membrane, having a higher IEC value and hence higher proton conductivity, showed significantly better fuel cell performance without any optimization. The achievable power density of our membrane outperformed Nafion by 150% under the testing conditions. This is presumably due to the higher proton conductivity of the sPFPE−SS membrane under the testing conditions, which helps to decrease the overall resistance of the MEA. Moreover, high levels of hydration were not as necessary for the MEA fabricated from the high IEC sPFPE−SS membrane relative to MEAs fabricated from Nafion 117.

3.6. High Surface Area PEMs. The lack of processability of commercially available PEMs has curtailed fabrication strategies, forcing all conventional PEMs to be flat and smooth at the surface. Such a two-dimensional configuration sets an upper limit on the active surface area of fuel cells and therefore limits the power density that is ultimately achievable in fuel cells, in addition to other issues such as transport phenomenon. Therefore, a high surface area three-dimensional interface between the PEM and catalyst layer is highly desirable. Patterned PEMs with unprecedented levels of morphologic control can be achieved easily using liquid precursors to fabricate PEMs by micromolding/imprint lithography techniques. Our liquid precursor materials were cast onto patterned sacrificial templates made from poly(cyanomethyl acrylate) films which were themselves patterned by soft-lithography techniques using an α,ω-methacryloxy-functionalized PFPE mold.[20] Figure 7a−c shows the SEM images of the patterned membranes with different aspect ratios. In the patterned membranes, the dimen-

sions of the square features are $3 \times 3 \times 1.4$, $3 \times 3 \times 1.9$, and $3 \times 3 \times 3.7$ μm, respectively. By employing soft lithographic techniques, the surface area of the patterned PEMs can be increased in a systematic manner through the generation of high-fidelity patterned PEMs. To investigate the effect of surface area on the power output of fuel cells, MEA performance was evaluated for both the flat as well as for the patterned PEMs with an IEC value of 1.50 mequiv/g and a thickness of 190 μm under identical test conditions. To exploit the surface area effect, ELAT electrodes could not be used with the patterned PEMs, since they too are flat. Therefore, a catalyst ink was formulated based on 20 wt % Pt/C catalyst, 5 wt % Nafion dispersion, and water. A 5 cm^2 test fixture was used in the fuel cell test system and as such the flat membrane system had an identical surface area to the test cell, but the patterned PEMs had calculated surface areas of 7.3, 8.3, and 11 cm^2, respectively, all within the 5 cm^2 test cell area. On the basis of the geometric surface area, a Pt loading of 0.2 mg/cm^2 was applied to all the membranes. For the flat membranes, the actual Pt loading was also 0.2 mg Pt/cm^2, since the actual surface area was equal to the geometrical area. For the patterned membranes, the actual Pt loading was much lower at 0.13, 0.12, 0.09 mg Pt/cm^2, respectively.

The MEA performance of the flat and patterned membranes was measured at 50 °C and 75% RH, and the results are compared in Figure 7d,e. As shown in Figure 7d, all of the patterned membranes show much better performance than the flat PEMs. When the cell potential was greater than 0.5 V, the MEA performance was found to be closely proportional to the surface area of the PEM membranes, with the higher surface area PEMs displaying better performance. At the higher current density region where the cell potential was lower than 0.5 V, a mass transfer limitation was observed, presumably due to flooding, which diminished the value of enhancing the PEM surface area. Under the test conditions, a power density as high as 225 mW/cm^2 was obtained for the patterned PEM, while that of the flat one was only 127 mW/cm^2. At a current density of 360 mA/cm^2, the MEA made from a flat PEM displayed a power density of 127 mW/cm^2, while the power density of MEAs made from patterned PEMs was measured to be 188, 199, and 204 mW/cm^2, respectively, which is 1.48, 1.57, and 1.61 times of the flat one. Due to the higher membrane thickness, unoptimized electrode preparation, and milder operation conditions, such power densities are not as high as some published results for thinner membranes, but it is important as a proof of concept. The power density obtainable increased in an almost linear fashion as a function of surface area, except for the membrane with a surface area of 11 cm^2. We believe the nonlinear relationship seen is due to the lower catalyst loading for the higher surface area membranes. Nonetheless, the higher surface area PEMs clearly result in higher power output of the fuel cells with the same geometric size. Therefore, the same power generation requirement can be achieved from a much smaller fuel cell stack composed of the patterned membranes than that composed of conventional flat membranes. This can potentially miniaturize fuel cells and promote their application in portable devices.

4. Conclusions

A series of novel fluoropolymer PEMs have been prepared from 100% solventless liquid precursors that are chemically cured into a network. By employing chemical cross-linking, high acid containing PEMs with proton conductivity much higher than that of Nafion have been obtained without the loss of mechanical integrity typical with linear polymers. The thermal stability of these materials is expected to be sufficient for fuel cell operations. To improve the long-term stability of the partially fluorinated material, sPFPE−SS membranes were fluorinated by elemental fluorine gas. The fluorinated PEM displayed higher decomposition temperature than the unfluorinated samples. The thermal and mechanical behavior of the sPFPE−SS PEMs were studied by DMTA and Instron instrument.

Properties such as water content, dimensional change, and proton conductivity were strongly related to the IEC of the new PEM materials. High acid content resulted in higher water uptake and better conductivity. High IEC sPFPE−SS membranes displayed better MEA performance than Nafion 117 under low water availability and mild operation conditions. By using imprint lithographic techniques, patterned PEMs with micron-sized features were easily fabricated with high fidelity. The patterned PEMs provided a much larger active surface area and therefore increased power density over standard PEMs. This can potentially miniaturize fuel cells and promote their application in portable devices.

This liquid precursor approach also provides many opportunities for fuel cell development that would be otherwise impossible. To improve the performance of direct methanol fuel cells, trilayer membranes with centered methanol barrier layers have been proposed.[41] By spin-coating and curing liquid precursors with different IEC values layer by layer, PEMs with controllable gradient in ion content and virtually continuous changing properties can be obtained with good adherence between the layers. Highly conductive 100% curable liquid precursors may also be used to replace solvent-based dispersions used for catalyst ink formulations and should afford enhanced interfacial contact. Moreover, liquid precursors to PEMs should also provide the possibility to fabricate MEAs with tailored interfacial properties by injection molding of liquid PEM precursors between preassembled electrodes. These possibilities are currently under investigation.

Acknowledgment. We gratefully acknowledge Dr. Lei Zhang for his invaluable help with SEM and Prof. Sergei Sheiko's group for use of Zeiss optical microscope and AFM. We thank Dr. Ginger M. Denison, Ms. Erin W. Dunn, Dr. Junhoe Cha, Ms. Elizabeth M. Enlow, and Ms. Jennifer Y. Kelly for their help and discussion. We would like to thank Department of Energy (5-35908) and NSF Science and Technology Center (5-37503) for financial support of this project and we acknowledge partial support from the Office of Naval Research (5-35747).

JA064391E

(41) Si, Y.; Lin, J.-C.; Kunz, H. R.; Fenton, J. M. *J. Electrochem. Soc.* **2004**, *151*, A463−A469.